



MINISTRY OF TECHNOLOGY

AERONAUTICAL RESEARCH COUNCIL

CURRENT PAPERS

The Effect at $M=1.7$ of
Removing Swept Endwalls
from a Wedge Compression Intake

by

M. M. Shaw

LONDON HER MAJESTY'S STATIONERY OFFICE

1968

SIX SHILLINGS NET

Comments on:

The Effect of at $M = 1.7$
of Removing Swept End Walls
From a Wedge Compression Intake

M. M. Sibley
 RAE Technical Report 68078
 March 1963

Presented in this paper are experimental data on a 10° single wedge supersonic intake with turning at the cowl lip tested in the RAE $3^\circ \times 3^\circ$ tunnel at $M = 1.7$. The intake was bifurcated and side mounted on a single engine combat aircraft fuselage, the short diffuser duct being roughly two compressor face diameters long. A fuselage boundary layer diverter and intake throat bleed slot were provided.

Tests were made at zero incidence and fixed wedge geometry with and without end walls the bottom end wall being removed first. Calibrations with and without throat bleed were made in each case, measuring mean pressure recovery, a compressor face flow distortion parameter and local total pressure distribution half-way along the duct.

This is an ad hoc test of a model arising from an aircraft project and results are presented in a manner intended to help the project designers. The beneficial effects on flow distortion of removing end walls and the significant influence of throat bleed on both recovery and flow distortion are brought out. The illustration in carpet form of local total pressure at the intermediate station is particularly useful and clearly shows the critical loss producing regions. The difficulty of preventing high order shock losses when the final shock in this case at $M = 1.343$ is sufficient to cause separation, is shown. The effect of sidewall removal is probably greatly influenced by the shock strengths and should not be generalised.

In defining the flow distortion characteristics it is unfortunate that high incidence and yaw conditions could not be covered although these are promised for a later date together with spillage drag figures. Whereas the mean pressure recovery is important at the steady design point, distributions are generally more critical at extremes of the flight envelope and are required to be known as early as possible. As a result many important questions governing the choice of an intake are unanswered.

In spite of these reservations this work undoubtedly provides valuable design information which, I think, would justify its publication as a Current Paper.

C.P. No.1026*
March 1968

THE EFFECT AT $M = 1.7$ OF REMOVING SWEEPED ENDWALLS FROM A
WEDGE COMPRESSION INTAKE

by

M. M. Shaw

SUMMARY

Mean pressure recovery, distortion and the extent of stable subcritical flow have been measured at zero incidence on a fuselage side intake having a wedge compression surface. The intake was separated from the fuselage by a boundary layer diverter, and had a bleed on the compression surface just inside the entry plane. It was tested with and without bleed having top and bottom swept endwalls on, top endwalls on, and both endwalls off.

Detailed measurements of duct total pressure were made at 1.8 times the capture height downstream of the inlet plane for all configurations.

Removal of the endwalls leads to an increase in the uniformity of pressure distribution and to an increase in the range of stable subcritical flow.

* Replaces R.A.E. Technical Report 68078 - A.R.C. 30569

CONTENTS

	<u>Page</u>
1 INTRODUCTION	3
2 MODEL AND TEST DETAILS	3
2.1 Model	3
2.2 Flow measurement and control unit	4
2.3 Reduction of data	4
2.4 Test conditions	5
3 RESULTS AND DISCUSSION	6
3.1 Pressure recovery, distortion and stable sub-critical range	6
3.1.1 Endwalls on, no bleed	6
3.1.2 Endwalls on, with bleed	6
3.1.3 Bottom endwalls off, no bleed	7
3.1.4 Bottom endwalls off, with bleed	7
3.1.5 Endwalls off, no bleed	8
3.1.6 Endwalls off, with bleed	8
3.2 Detailed pressure distribution	8
3.2.1 Endwalls on	8
3.2.2 Removal of endwalls	9
4 CONCLUSIONS	10
Symbols	11
Illustrations	Figures 1-19
Detachable abstract cards	-

1 INTRODUCTION

Aircraft intakes for operation at Mach numbers above about 1.4 are normally of the multiple shock type. That is to say they normally have one or more surfaces inclined at an angle to the main stream which compress the air in successive stages. These surfaces can either be axi-symmetric (conical or half-conical) or two-dimensional (wedges).

The description "two-dimensional" is not quite accurate, since the ratio of intake width to height is such that their behaviour can be quite sensitive to the end conditions. Unpublished work by Goldsmith demonstrates that a spillage of 5% in pressure recovery and 10% in critical mass flow is incurred by removing the swept endwalls from a wedge compression surface at $M = 2.5$.

The work described in the present paper investigates the effect of removing endwalls at a somewhat lower Mach number ($M_L = 1.7$). It was suspected that at zero incidence the performance penalties might be lower, or even non-existent, thus enabling the designer to use other criteria to determine whether or not swept endwalls should be provided.

The results of the experiment show that pressure recovery is virtually unchanged by removal of the endwalls. They show that the total pressure distribution in the duct becomes more uniform, and that the range of stable sub-critical flow is slightly increased. There is a small spillage of 2% of the critical mass flow.

Work on other aspects of this type of intake, for example the effects of incidence, and the magnitude of spillage drag, is being continued on a more suitable model.

2 MODEL AND TEST DETAILS

The aircraft on which the intake is mounted was represented externally to a short distance downstream of the plane of entry, and internally up to the engine face. The model was held in the wind-tunnel by means of a sting mounted assembly which incorporated flow measuring and controlling equipment.

2.1 Model

Fig.1 shows a photograph of the model and Fig.2 the duct shape. The 10° wedge compression surface was separated from the fuselage by a boundary layer diverter of 36° included angle, and a bleed was provided on the compression

surface just inside the entry plane. The fuselage shape was distorted behind the canopy to give room for the throat bleed ducts above the main intake duct. Figs.2 and 3 show the intake and duct geometry. The main duct was relatively short, highly curved, and had a slow rate of diffusion. There was some obstruction to the ends of the boundary layer bleed slot caused by the encroachment of the diverter air passages.

A pitot rake of twenty three tubes was placed in the starboard duct at a distance of 1.8 times the capture height behind the entry plane. Fig.4 gives details of the duct cross section at this rake station, and the positions of the pitots relative to the duct walls.

2.2 Flow measurement and control unit

A general arrangement of the sting and the measuring cell is given in Fig.5. The sting carried the main mass flow control and measuring unit which in turn carried the bleed mass flow control and measuring unit. The model was placed in front of these units. Engine face pressure recovery was measured by a rotatable cruciform rake of twenty four pitot tubes. For most of the test this rake was placed at 15° to the plane of symmetry, but a small number of measurements was made in which the rake was moved 15° at a time to give a detailed survey of 144 points over the engine face. Four wall statics were placed one diameter downstream of the engine face pitots, and four more one and a half diameters further downstream, half way to the exit.

The bleed flow control and measuring unit operated on the port and starboard ducts simultaneously. Each duct contained three pitot tubes and four wall statics at the same longitudinal station.

2.3 Reduction of data

The engine mass flow was calculated by the "choked exit method" in which the geometrical exit area is assumed to be the area at which the local Mach number is unity, and the total pressure just upstream of the exit is calculated from the ratio of the duct area to the exit area in combination with the measured static pressure, as given by the equations below

$$\frac{A_\infty - A_{bl}}{A_{en}} = \frac{P_v}{P_T} \cdot \left(\frac{A}{A^*}\right)_\infty \cdot \frac{A_{ex}}{A_{en}} \quad \text{where } P_v = f\left(p_v, \left(\frac{A^*}{A}\right)_v\right),$$

the suffix v relates to the constant area duct in which static pressure is measured, A_{en} denotes the intake entry area, and P_T the free stream total

pressure. The discharge coefficient at the exit was assumed to be unity throughout.

The choked exit method did not give plausible results when it was applied to the calculation of bleed flow, so the mass flow through the bleed ducts was calculated from the area of the duct and the Mach number in it obtained by pitot and static readings.

$$\frac{A_{bl}}{A_{en}} = \frac{P_d}{P_T} \frac{A_d}{A_{en}} \left(\frac{A}{A^*}\right)_{\infty} \left(\frac{A^*}{A}\right)_d$$

where the suffix d refers to the bleed measuring station. $\left(\frac{A^*}{A}\right)_d$ is of course a known function of the measured Mach number there.

All the total pressure tubes were placed to govern equal areas so that the calculations of area weighted pressure recovery reduce to the calculation of the arithmetic mean.

Area weighted mean pressure recovery $\frac{P_A}{P_T}$ or $\frac{P_R}{P_T} = \frac{1}{n} \frac{\sum_{i=1}^n P_i}{P_T}$ where P_i are the individual pitots either at the engine face or in the intake duct.

The mass flow weighted mean pressure recovery uses the mean static pressure one diameter downstream of the compressor face in combination with the individual pitots to work at local mass flows, and the expression to calculate P_M is given below:-

$$P_M = \frac{\sum P_i^2 \left(\frac{A^*}{A}\right)_i}{\sum P_i \left(\frac{A^*}{A}\right)_i}$$

2.4 Test conditions

The model was tested in the 3ft x 3ft wind-tunnel at R.A.E. Bedford during February 1966. The Reynolds number based on capture height (Fig.2) was 0.21×10^6 .

Initial tests showed that the boundary layer was separating from the side of the body just in front of the intakes, and it was necessary before proceeding with the main series to prevent this. It was done by removing material from the nose at its widest point until observation of the flow in the schlieren beam showed the desired result. The schlieren photographs

(e.g. Fig.6c) show that most of the boundary layer was going underneath the 10° compression surface after this process had been completed.

3 RESULTS AND DISCUSSION

3.1 Pressure recovery, distortion and stable sub-critical range

3.1.1 Endwalls on, no bleed

Fig.6a gives the area weighted and mass flow weighted mean pressure

recoveries $\frac{P_A}{P_T}$, $\frac{P_M}{P_T}$ and the distortion parameter $\frac{V_{\max} - V_{\min}}{V_{\text{mean}}}$ plotted

against intake mass flow. Difficulties of measurement were encountered in this configuration. The flow was not very steady, making it difficult to recognize the precise mass flow at which buzz set in, and causing the manometers to move rather unpredictably. The results show that high distortions

were present $\left(\frac{V_{\max} - V_{\min}}{V_{\text{mean}}} \approx 1.3 \right)$, that the assumption of constant dis-

charge coefficient of unity at the exit broke down in the supercritical region, and perhaps before, and that pressure recovery levels were low.

The difference between mass flow weighted pressure recovery and area weighted pressure recovery is 0.04; this difference is due to the fact that mass flow weighted pressure recovery gives less importance to areas of low mass flow (i.e. low pressure recovery). The larger the discrepancy between the two values, the worse the distortion must be, and we note that

$0.04 \left(= \frac{P_M - P_A}{P_T} \right)$ goes with $\frac{V_{\max} - V_{\min}}{V_{\text{mean}}} = 1.3$. Both these parameters show

that the flow at the compressor face is far from uniform, and that the intake is not performing satisfactorily.

3.1.2 Endwalls on, with bleed

Fig.6b shows an improvement of 0.07 in critical pressure recovery attributable to about 4% bleed flow. The reduction in distortion

$\frac{V_{\max} - V_{\min}}{V_{\text{mean}}}$ to 0.5 and the difference between $\frac{P_M}{P_T}$ and $\frac{P_A}{P_T}$ of only 0.005 are

other indications of the improvement. The very short stable subcritical range is noteworthy. When the bleed flow is just able to control the shock induced separations, as here, the onset of buzz can be sudden and the amplitude large

at a very slightly lower mass flow than the stable condition. This type of behaviour is contrasted with that described in the previous section where some unsteadiness was present for most of the so-called stable subcritical range.

The photograph of Fig.6c shows that the wedge shock is at 47° to the local flow direction which indicates a local flow Mach number of 1.7.

This gives a maximum theoretical flow into the intake (ignoring sideways spillage) of:-

$$\left(\frac{A_L}{A_{en}}\right)_{\max} = \frac{\cot \theta_\ell - \cot \delta}{\cot \theta_W - \cot \delta} = 0.943 \quad ,$$

where the suffix L indicates local conditions, and A_L is the area of the entry stream tube at M_L , or

$$\left(\frac{A_\infty}{A_{en}}\right)_{\max} = \left(\frac{A_L}{A_{en}}\right)_{\max} \times \left(\frac{A^*}{A}\right)_L \times \left(\frac{A}{A^*}\right)_\infty = 1.013$$

which agrees reasonably well with the measured value of 1.01. Also, the maximum value of pressure recovery recorded by the rakes (Figs.9 and 11) accords well with the level expected from a two shock recovery with a 10° wedge at $M = 1.7$. Additional evidence for this value of local Mach number is afforded by the angle of the Mach wave arising from a joint on the body seen on Fig.6c in front of the intake.

Duct mean pressure recoveries $\frac{P_R}{P_T}$ for this or the previous configuration are not available due to the presence of leaks during the early runs.

3.1.3 Bottom endwalls off, no bleed

The curves of pressure recovery and distortion of Fig.7a are of the type described in section 3.1.1, having high distortions and some unsteadiness over most of the subcritical range. However, the critical point is better defined and the distortions are not quite so high as they were when both endwalls were on.

3.1.4 Bottom endwalls off, with bleed

The addition of 4% bleed flow changes the behaviour of the intake as it did in section 3.1.2. There is a sharply defined end to the stable sub-

critical range at $\frac{A_\infty}{A_{en}} = 0.95$ whereas without bleed the unsteadiness

gradually increased. The stable range with bleed and with both endwalls

present ended at $\frac{A_{\infty}}{A_{en}} = 0.98$ showing, as in the last section that the

removal of a swept endwall improves the intake's performance.

3.1.5 Endwalls off, no bleed

$\frac{V_{max} - V_{min}}{V_{mean}}$ falls below 1.0 and the stable subcritical range extends to

$\frac{A_{\infty}}{A_{en}} = 0.91$. Area mean pressure recovery remains at 0.83 as with one endwall removed, and the discharge coefficient remains constant in the supercritical range.

3.1.6 Endwalls off, with bleed

The steady improvement in distortion and subcritical range as endwalls are removed and bleed is added continues (Fig.8b). Distortion reaches the lowest value measured in this experiment (0.2) with 4% bleed flow at

$\frac{A_{\infty}}{A_{en}} = 0.96$. The pressure recovery is greatest just before buzz occurs where it reaches 0.921, higher than in any of the other configurations tested.

Comparison of maximum mass flow with and without endwalls (Figs.6b and 8b) indicates that some 2% is spilling sideways when the endwalls are removed.

3.2 Detailed pressure distribution

3.2.1 Endwalls on

Figs.9, 10 and 11 give the total pressure distribution in the duct measured by the 23 rakes at the position shown in Fig.2.

At both $\frac{A_{\infty}}{A_{en}} = 0.87$ and 0.98 (Figs.9 and 10) the distribution without bleed on the compression surface is dominated by the large areas of separated flow adjacent to that surface. The effect of bleed at $\frac{A_{\infty}}{A_{en}} = 1.005$ (Fig.11)

is to reduce these areas by a considerable amount, although this bleed configuration is obviously less than fully effective at what may be a slightly

supercritical mass flow. In both these cases near $\frac{A_{\infty}}{A_{en}} = 1.0$ the recovery

rises to the theoretical shock recovery value at some point on all rakes except that next to the bottom.

Two of the five tubes in the rake just mentioned are known to be subject to leakage for this condition, and it is possible that some of the others were as well, with the result that the interpolations, shown dotted on Figs.9, 10 and 11 might be misleading.

3.2.2 Removal of endwalls

The effect of removing endwalls is threefold:-

- (a) the effect of the boundary layer on the endwall is removed;
- (b) the boundary layer on the compression surface is locally swept aside round the top and/or bottom of the intake;
- (c) this sideways spillage is accompanied by re-acceleration of the main flow into the intake so that the Mach number at which the normal shock occurs increases.

If the bottom endwall is removed these effects occur asymmetrically. Figs.13 and 14 show this quite clearly; pressures adjacent to the compression surface increase from top to bottom, and the opposite effect occurs adjacent to the cowl.

The far more symmetric patterns of Figs.16 and 17 illustrate the same points when both endwalls are removed. The pressure recovery of about 0.9 which occurs fairly consistently all over the duct outside the separated flow regions when both endwalls are removed or near the bottom of the duct when that endwall is removed indicates that the flow expands from a Mach number of 1.35 behind the 10° wedge shock when the endwalls are present to $M = 1.56$ and as was noted earlier this occurs when 2% of the flow is spilled sideways.

In Fig.17 at $\frac{A_\infty}{A_{en}} = 0.914$ the bleed flow is high and the normal shock is on or near the leading edge of the bleed. In Fig.18 the bleed flow is halved, consistent with the normal shock now being positioned on or possibly downstream of the bleed trailing edge so that separated regions re-appear adjacent to the compression surface. Fig.19 illustrates directly for those rakes nearest to the endwalls the truth of statements (a), (b) and (c) made above. In every case, whether boundary layer bleed is present or not, and independently of the precise mass flow ratio the boundary layer on the compression surface with endwalls on is thicker, and the pressure recovery near the cowl is higher. The latter effect is of course due to the lower Mach number at which the flow enters the intake compared with its value with endwalls removed.

Thus the effect of removing endwalls on overall pressure recovery is very small, the higher shock losses almost exactly balancing the reduced viscous losses, but there are advantages as regards more uniform flow into the intake which are repeated as better distributions at the engine face.

4 CONCLUSIONS

The performance of a fuselage side intake with a 10° wedge compression surface has been measured at a local Mach number of 1.7. Pressure distributions in the diffuser have indicated reasons for the change in performance due to the removal of swept endwalls from the wedge compression surface.

It has been found that removal of the endwalls leads to an improvement in uniformity of pressure distribution and a small increase in stable sub-critical flow.

SYMBOLS

A_{bl}	area of free stream tube entering bleed ducts
A_{en}	capture area of intake
A_{ex}	exit area of measuring unit
A_c	area at compressor face
A_v	area at station v ($1\frac{1}{2}$ diameters upstream of exit)
A^*	throat area corresponding to Mach number at station indicated by suffix
A_{∞}	area of free stream tube entering intake ($M_{\infty} = 1.8$)
P	mean total pressure
P_T	tunnel total pressure
P_A	area weighted mean total pressure
P_M	mass flow weighted mean total pressure
P_R	area weighted mean total pressure in intake duct
p	mean static pressure
p_c	mean static pressure at station half a diameter downstream of compressor face rake
p_v	mean static pressure at station v
δ	angle of wedge compression surface to free stream
θ_w, θ_c	complement of shock and endwall sweepback angles

Other suffices

d	bleed duct measuring station
∞	free stream conditions ($M_{\infty} = 1.8$)
L	local conditions ($M_L = 1.7$)

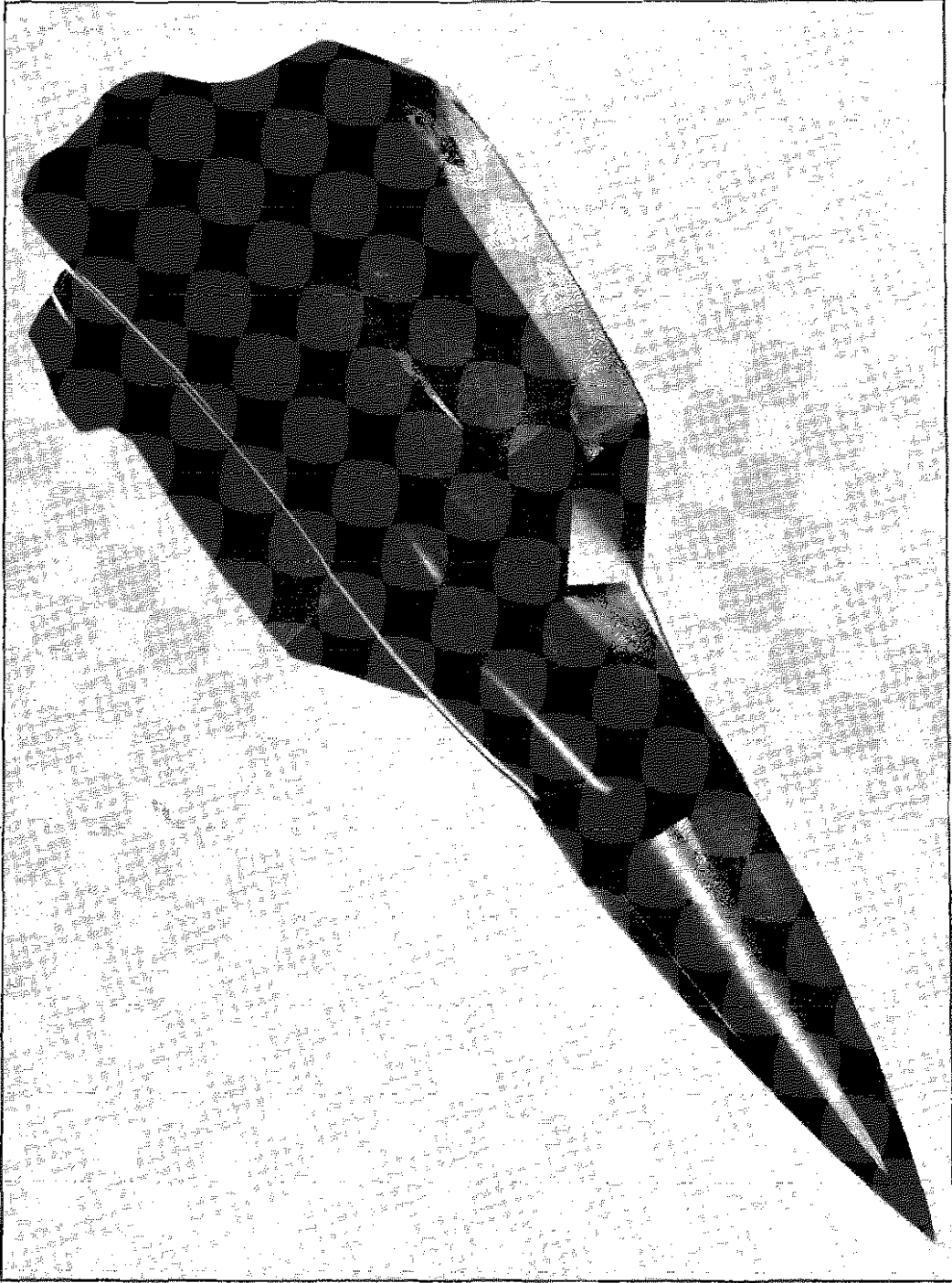


Fig.1 Model with swept endwalls

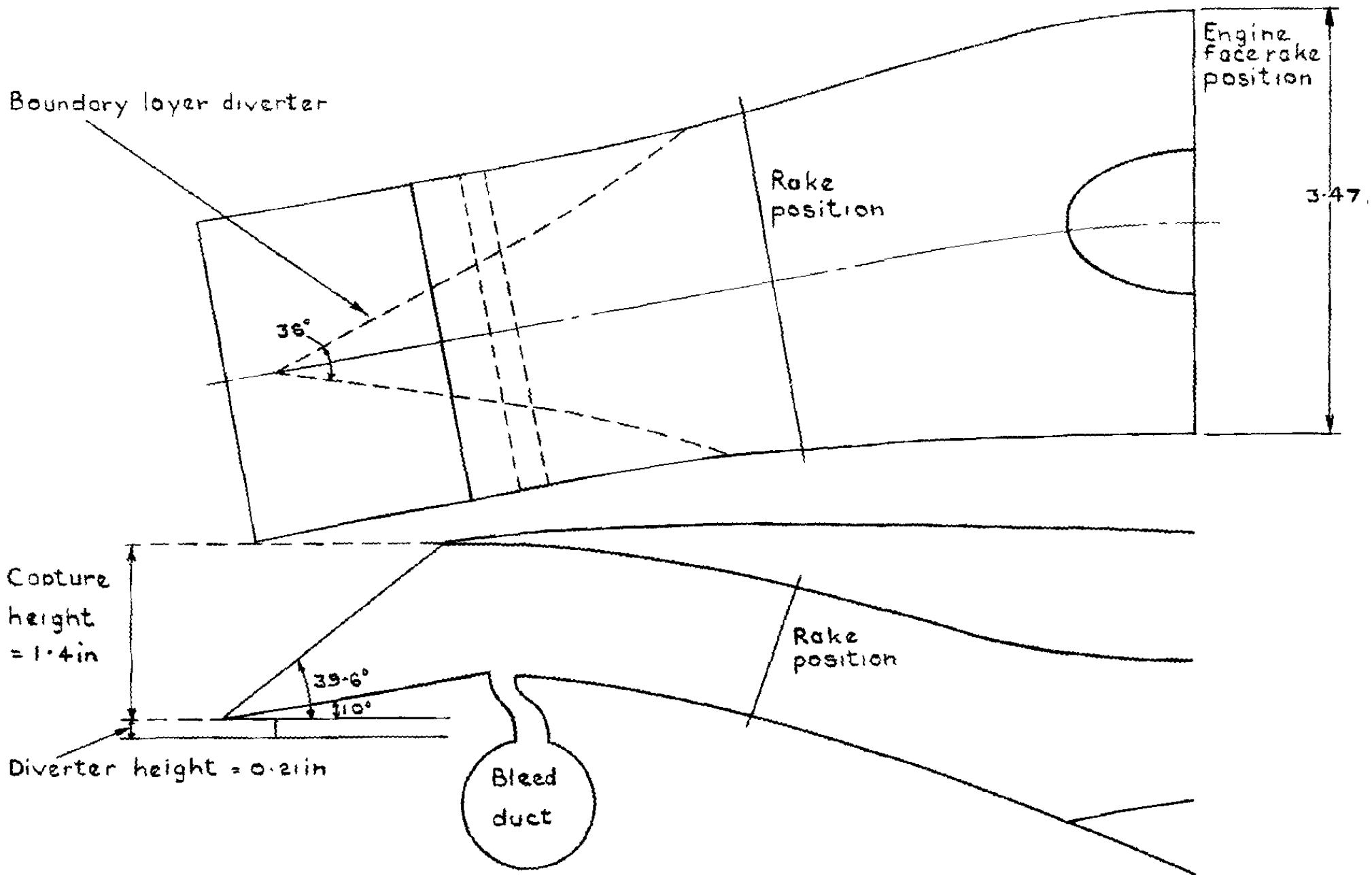


Fig.2 Duct shape, very nearly model scale

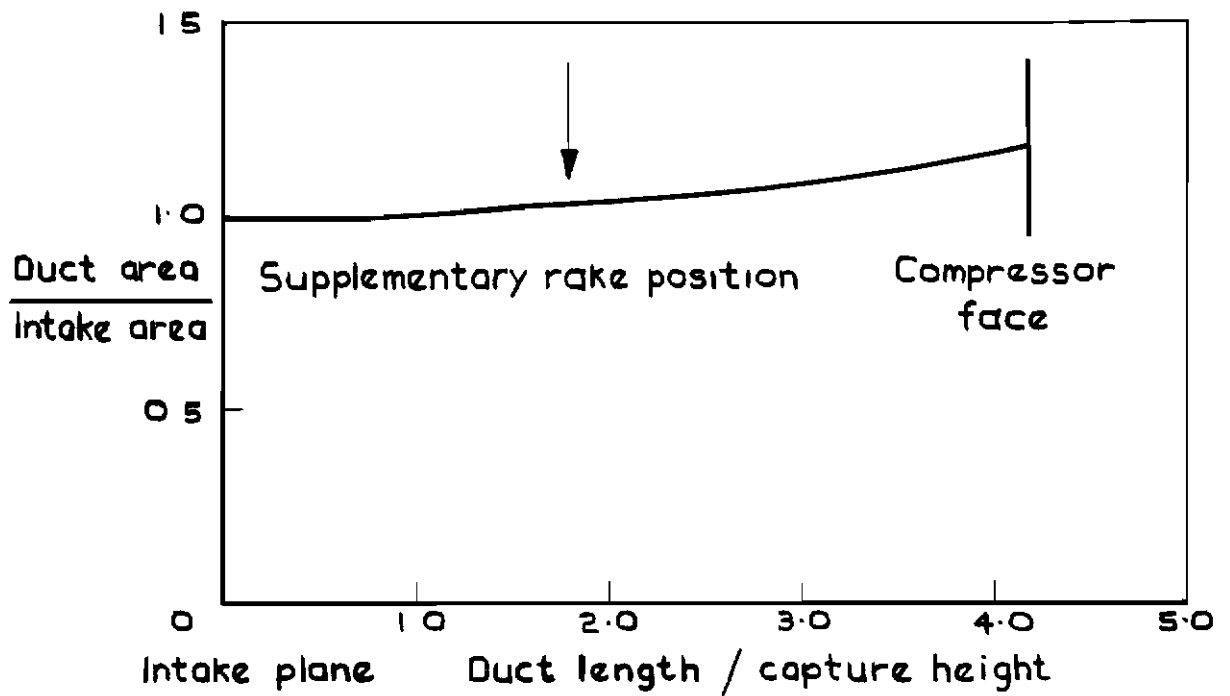


Fig. 3 Duct area distribution

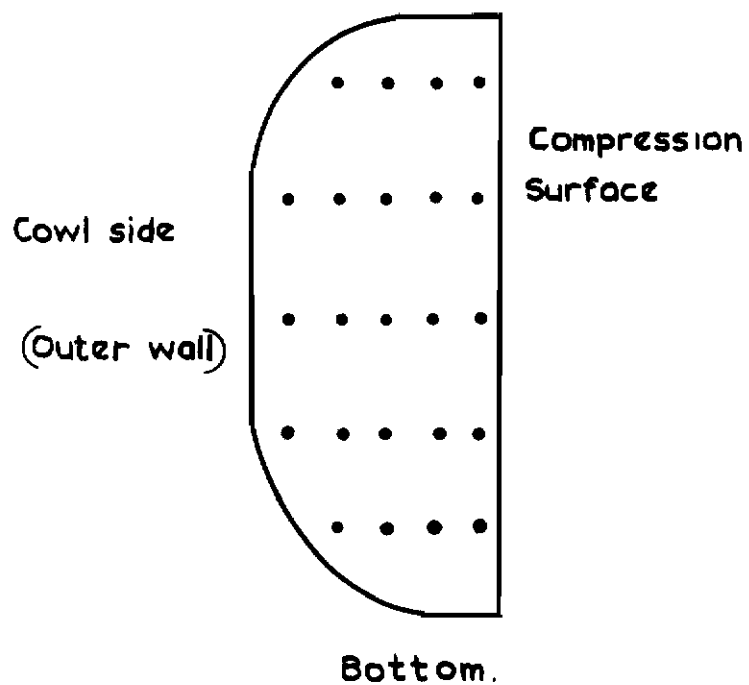


Fig. 4 View of supplementary pitot rake from the front.

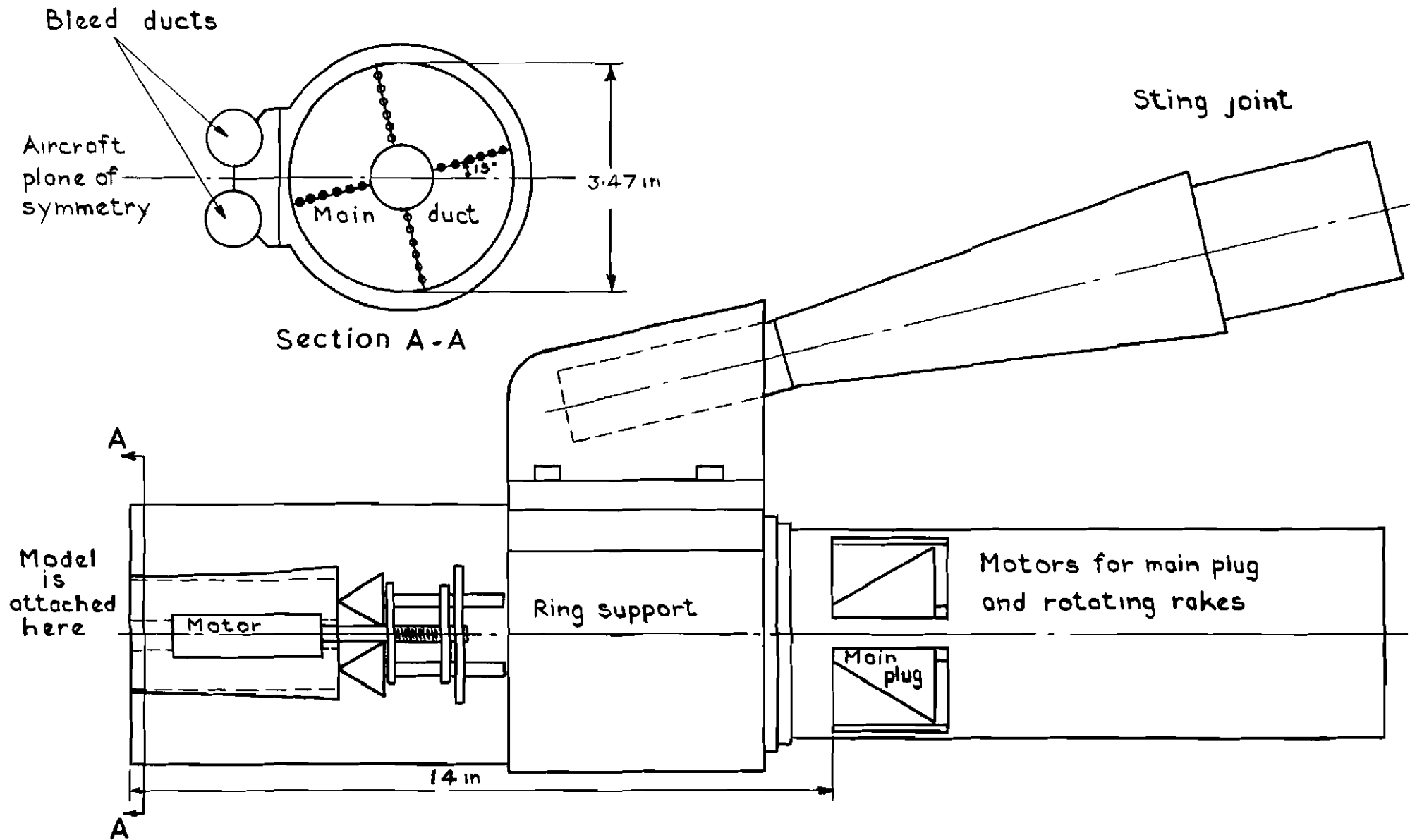
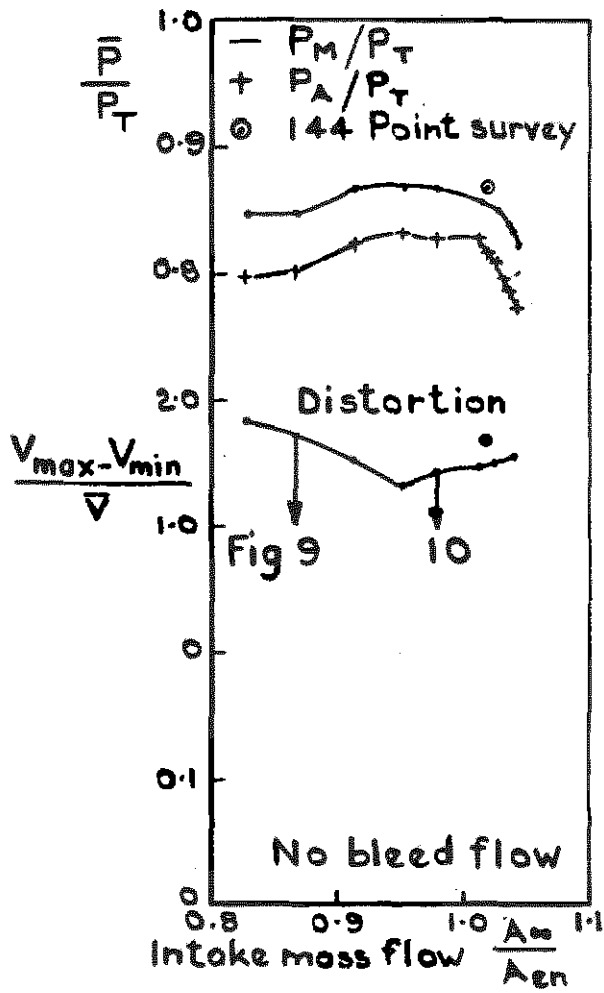
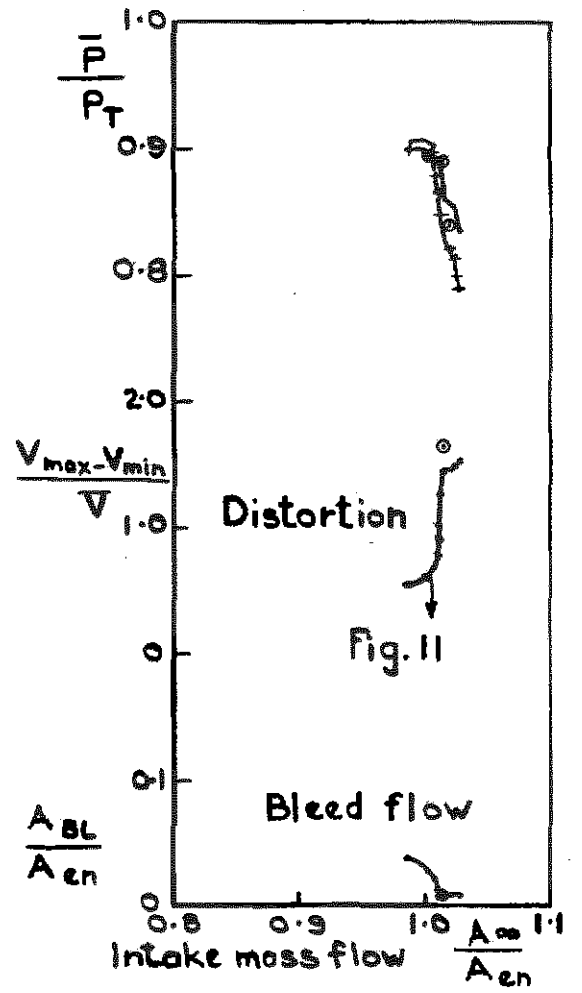


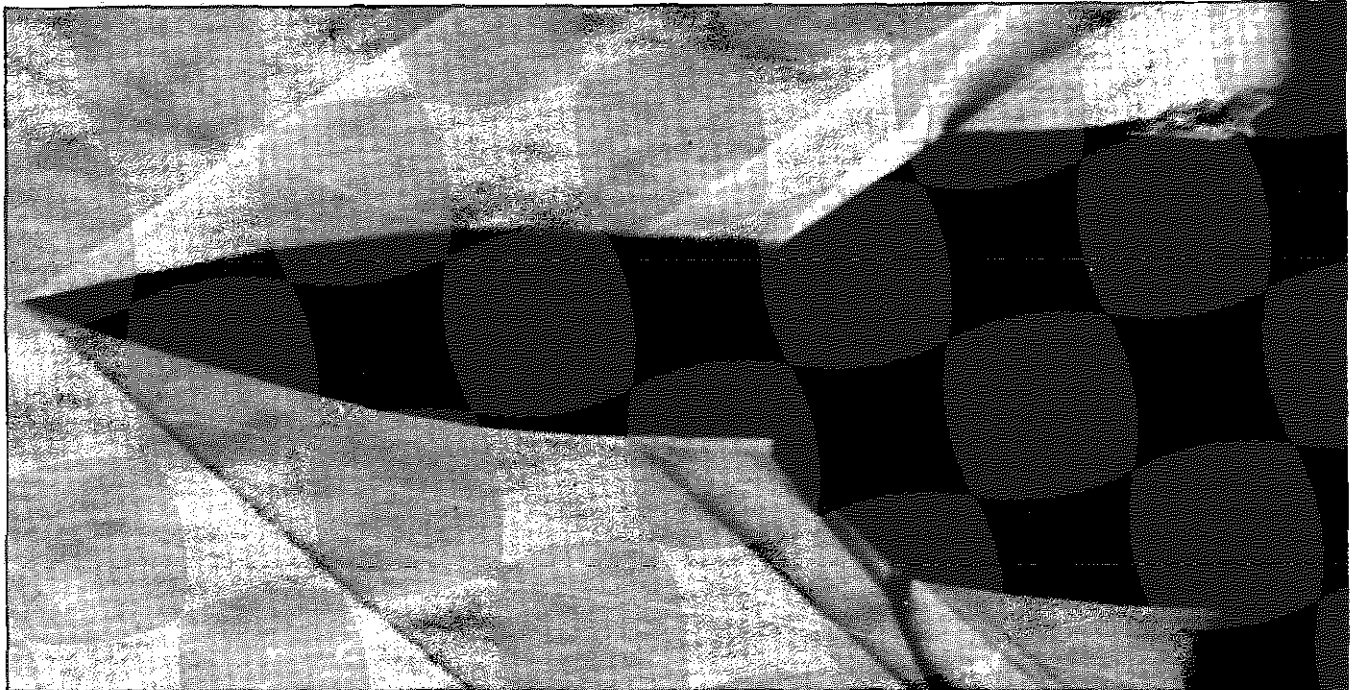
Fig.5 Main cell, bleed plugs and sting support



(a) No bleed

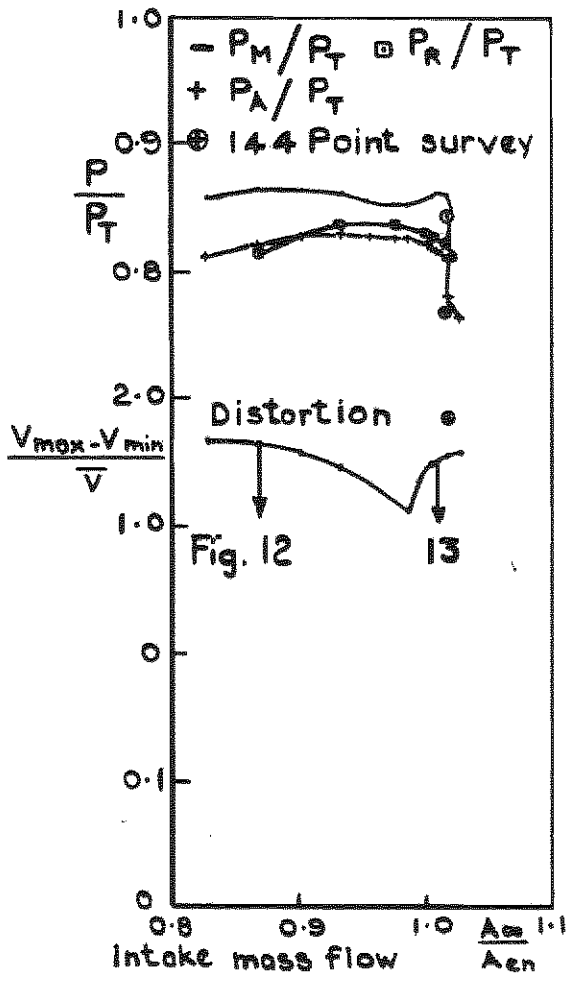


(b) With bleed

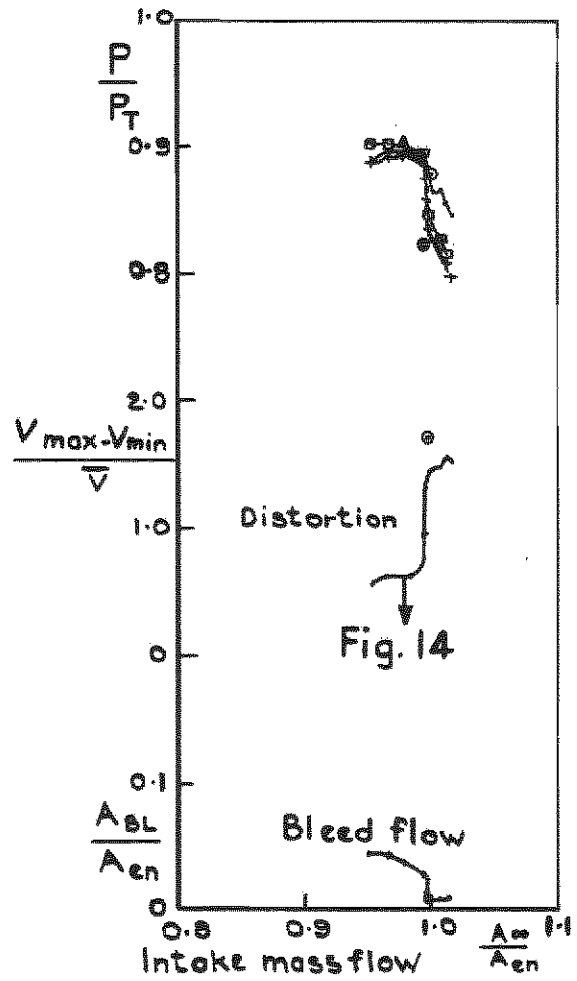


(c) Minimum stable flow no bleed

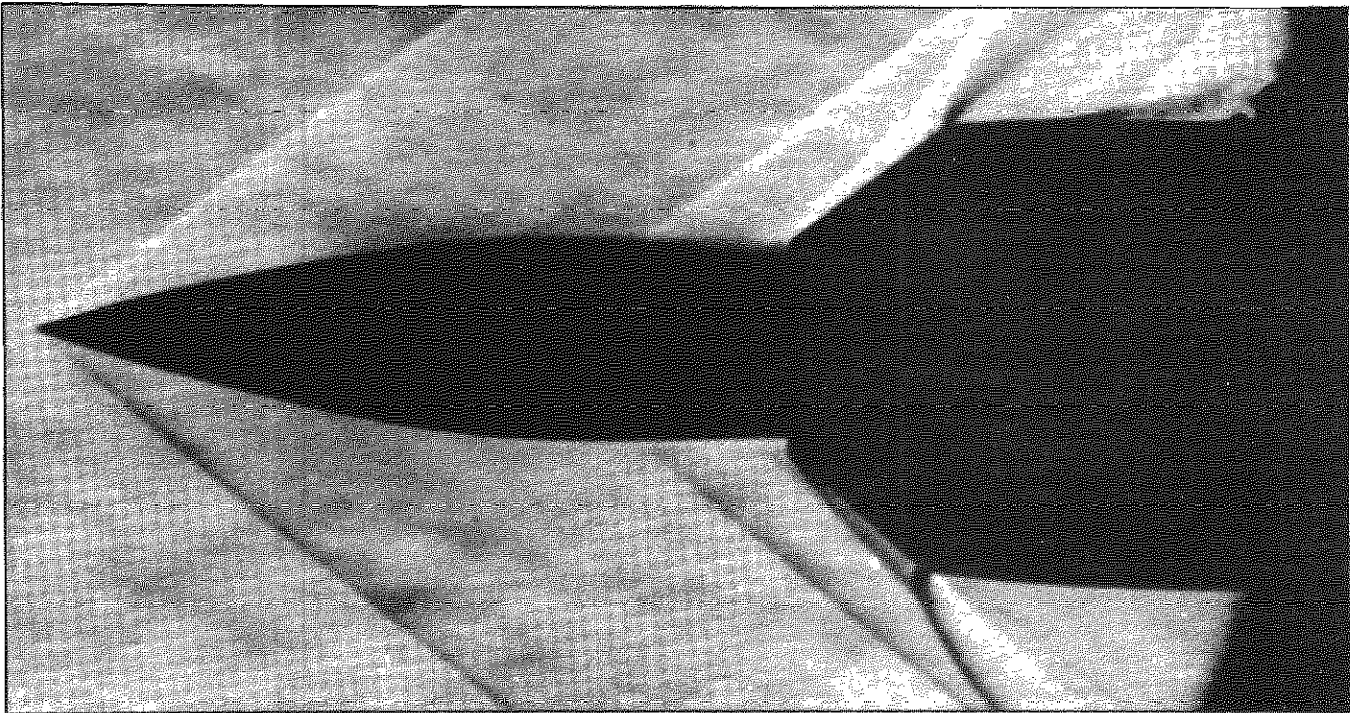
Fig.6 Endwalls on



(a) No bleed

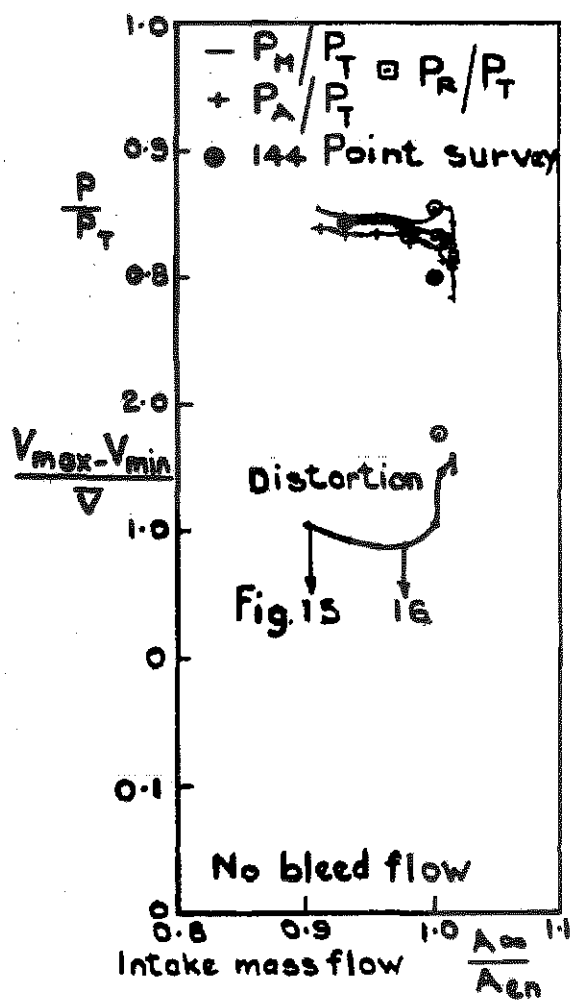


(b) With bleed

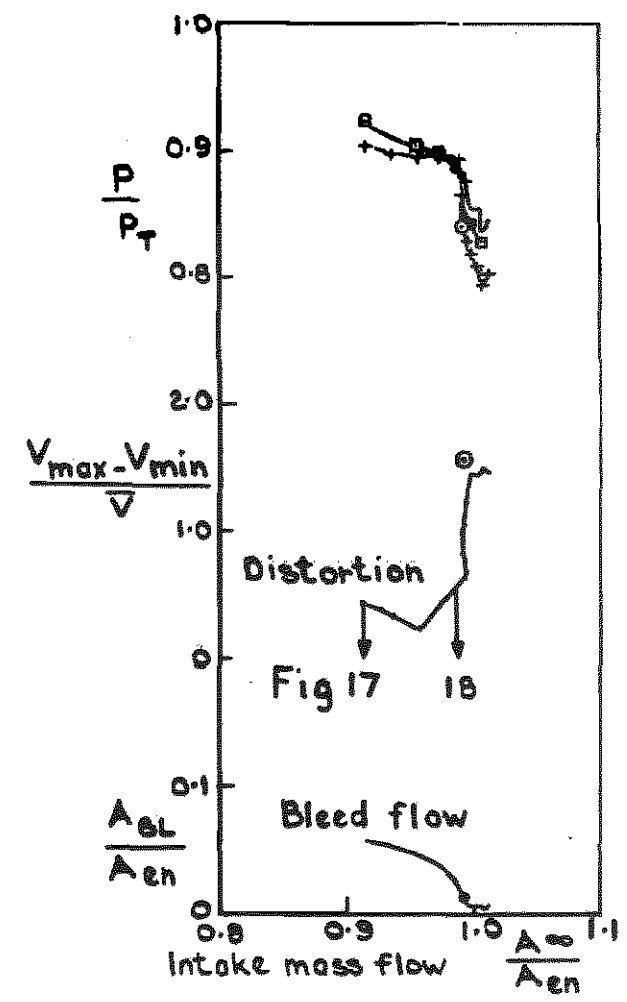


(c) Critical point, no bleed

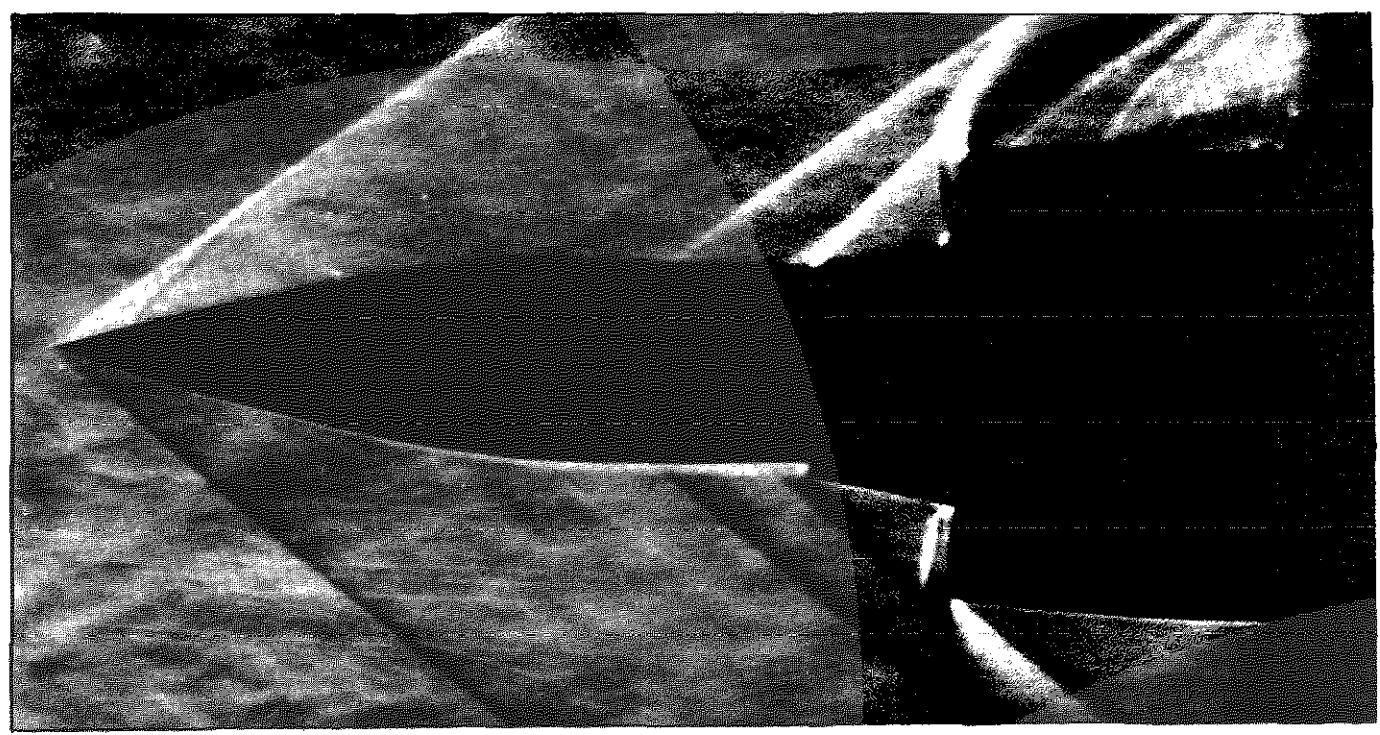
Fig.7 Endwalls removed from bottom



(a) No bleed



(b) With bleed



(c) Minimum stable, with bleed

Fig.8 Endwalls removed

NB. Note false origin

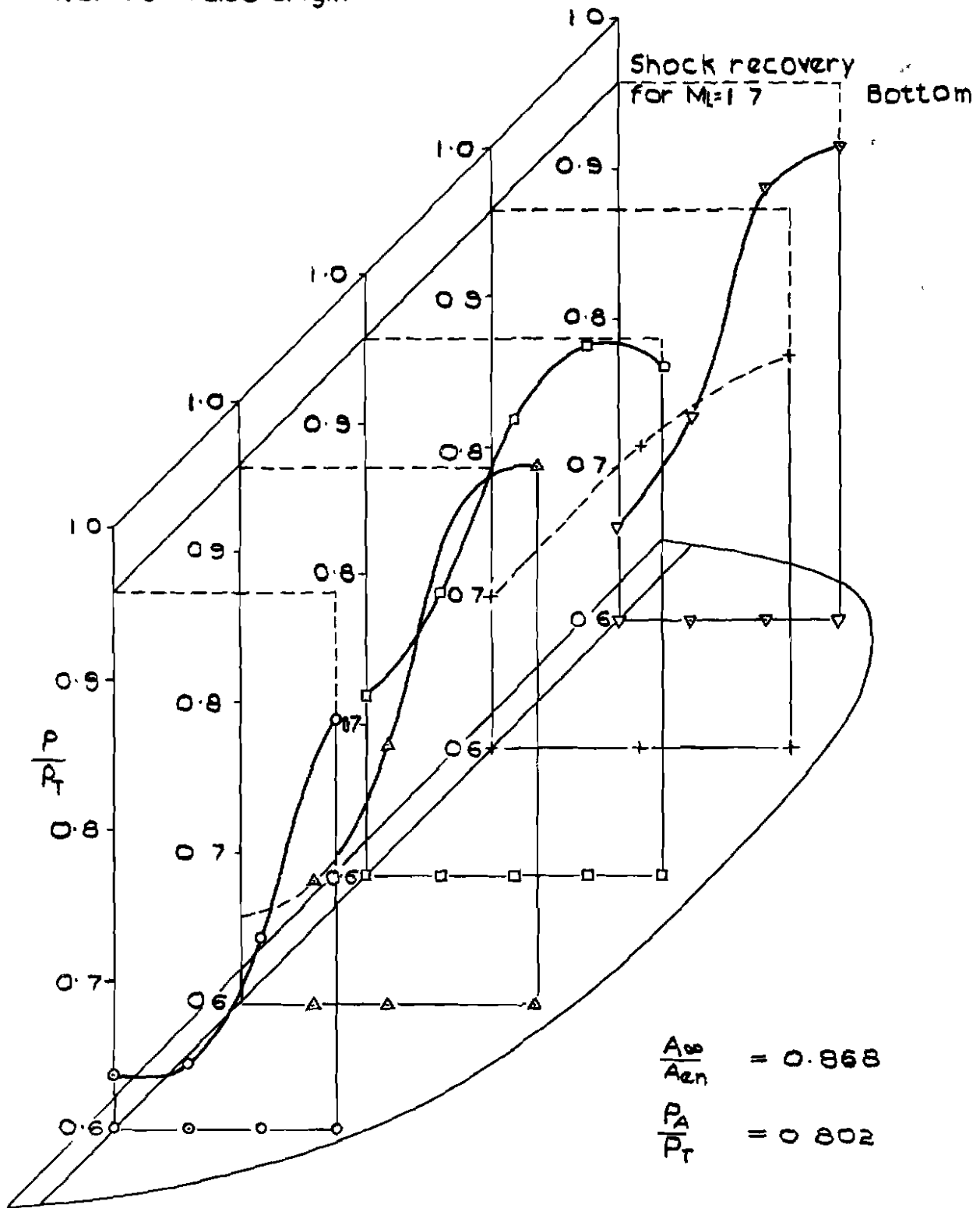


Fig 9 Duct pressure distribution endwalls on, no bleed.

N.B. Note false origin

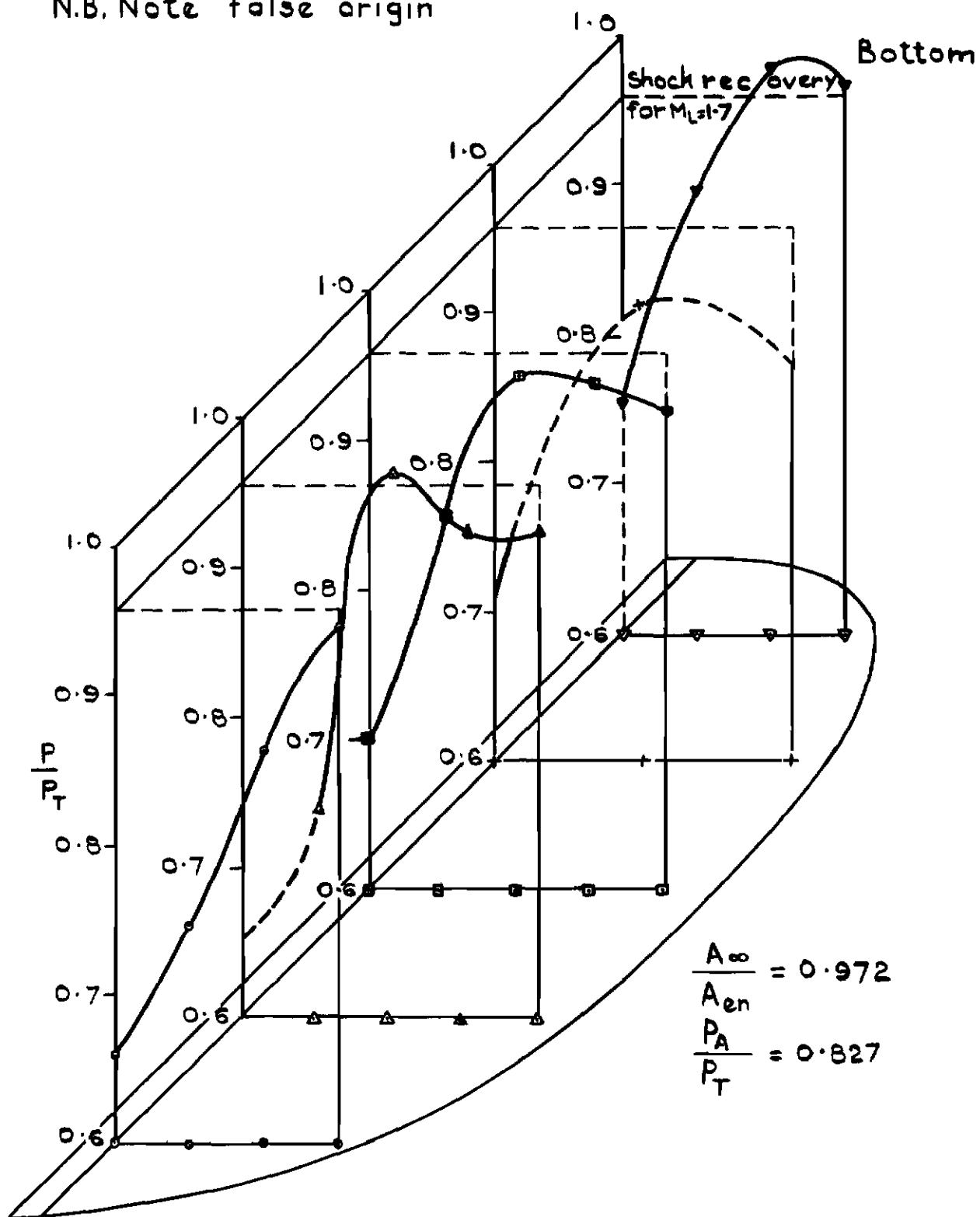


Fig.10 Duct pressure distribution endwalls on, no bleed.

NB Note false origin

Bottom

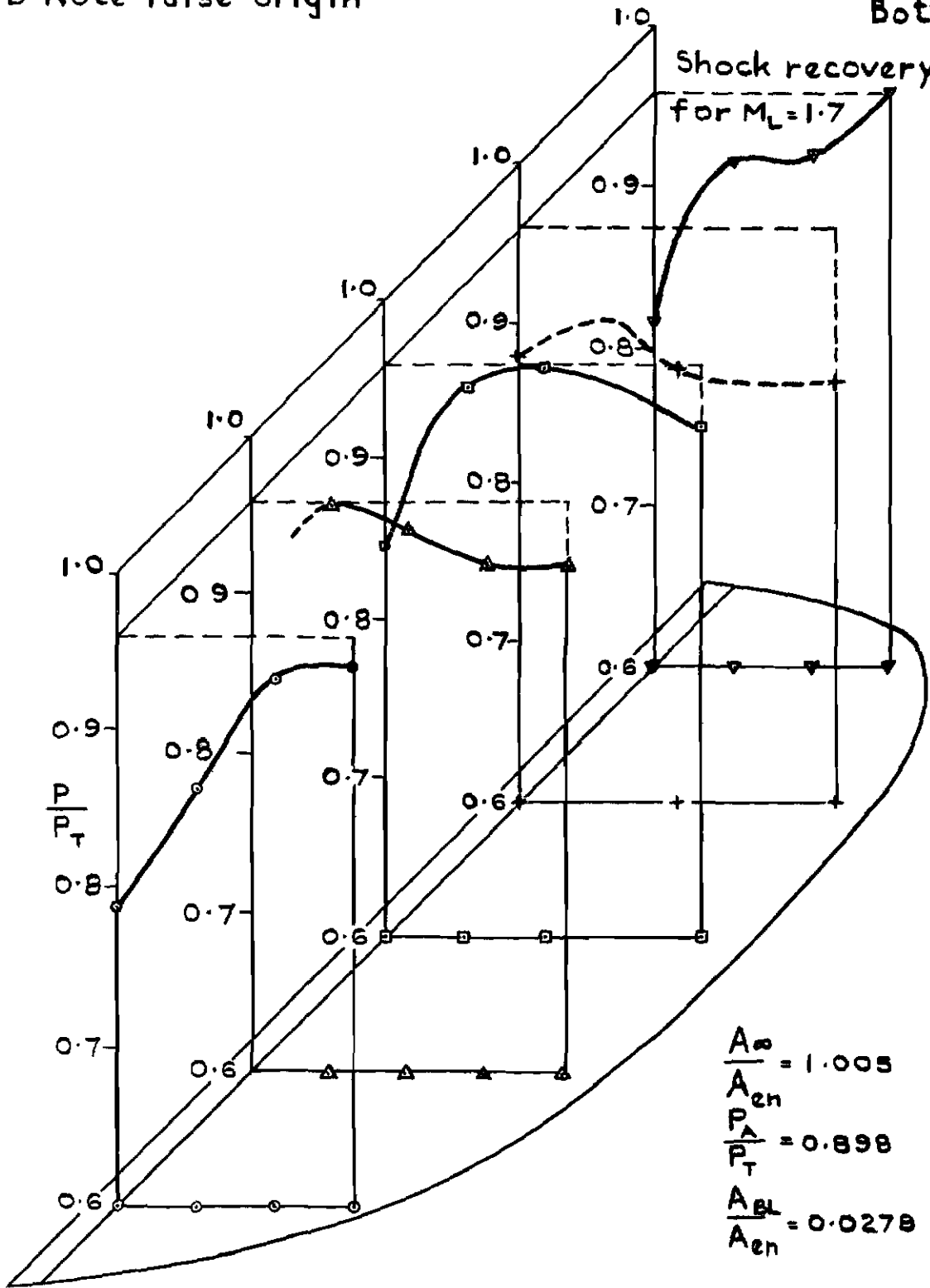


Fig.II Duct pressure distribution endwalls on, with bleed.

NB Note false origin

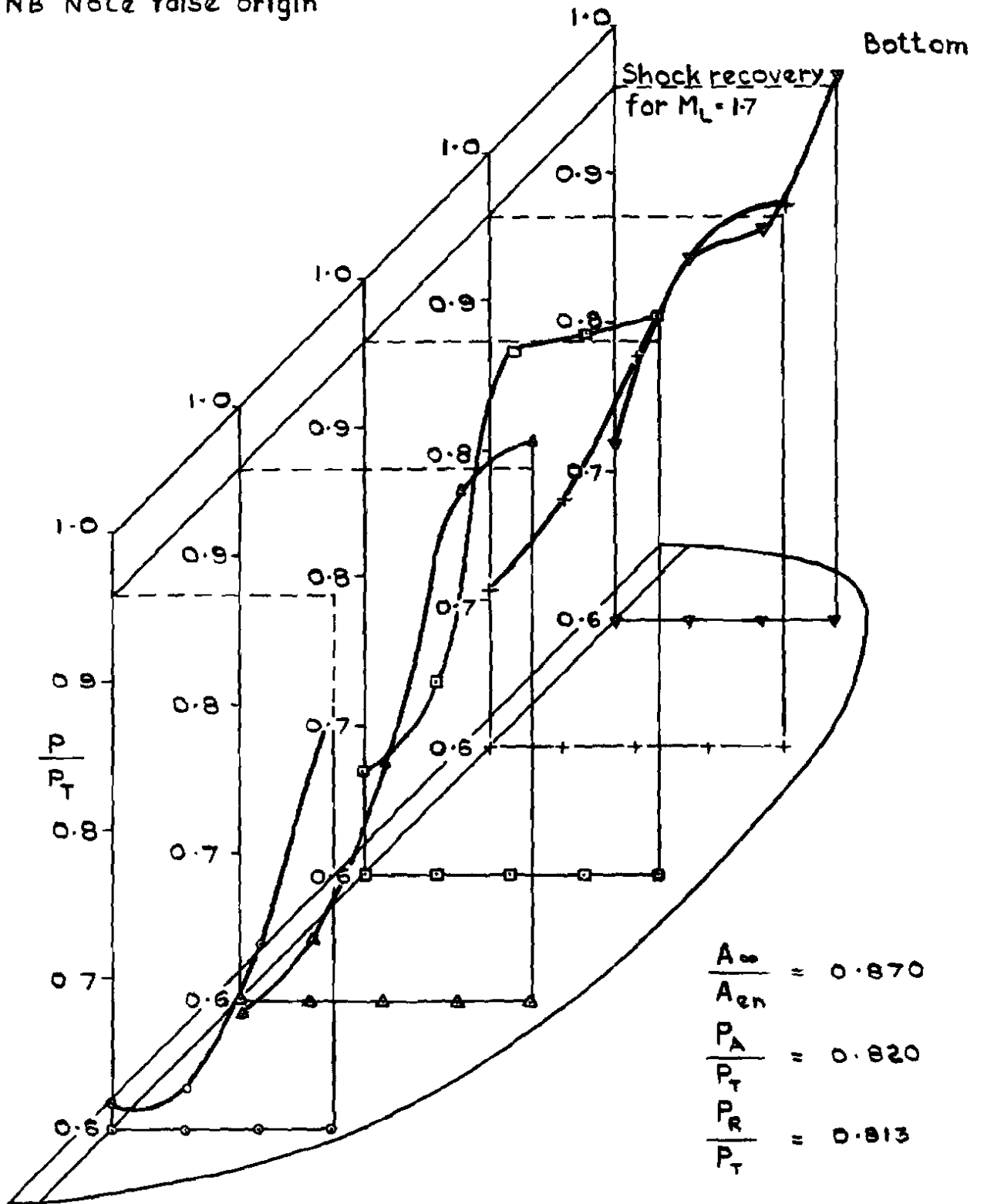


Fig.12 Duct pressure distribution.
endwalls removed from bottom, no bleed.

NB Note false origin

Bottom

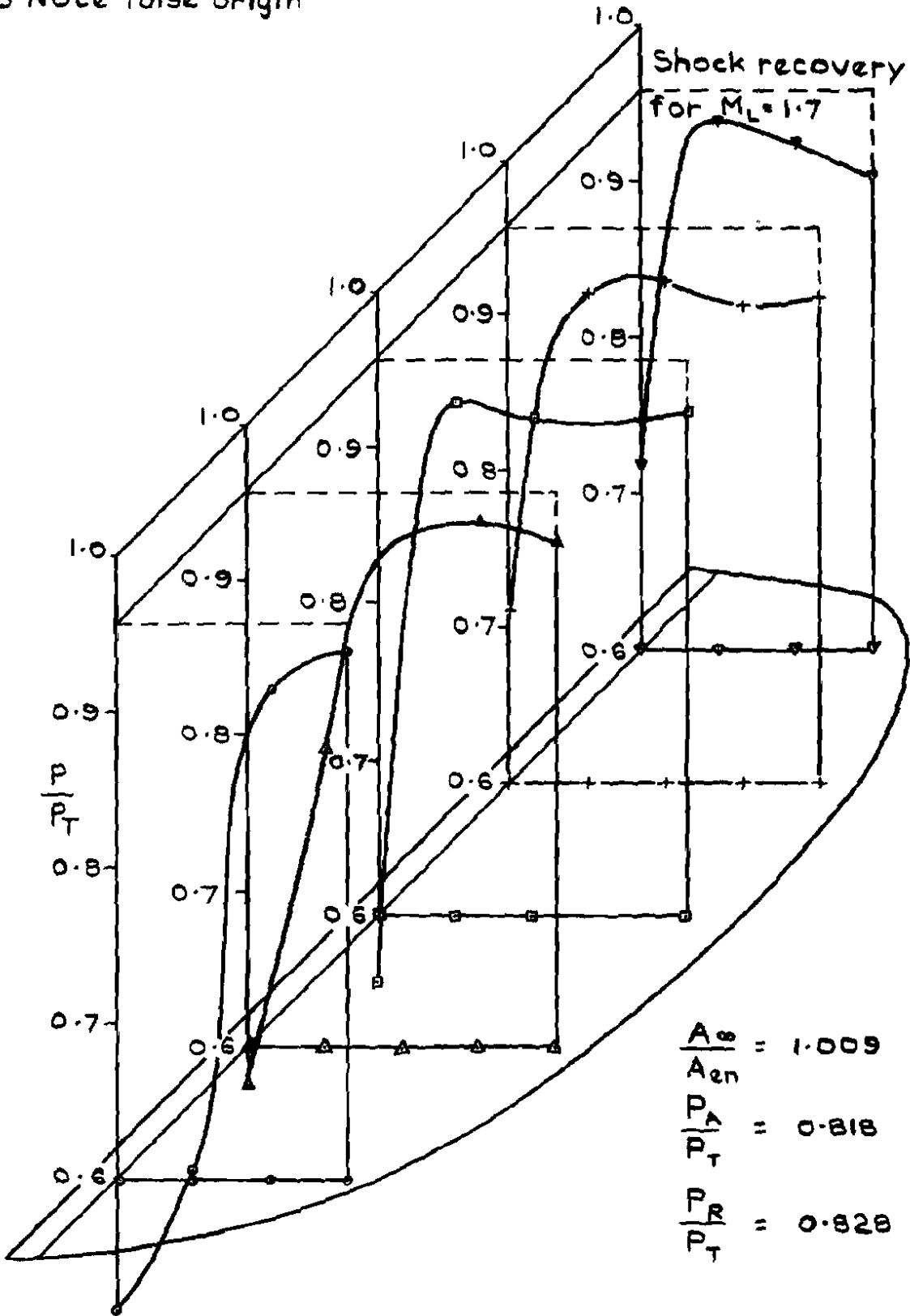


Fig.13 Duct pressure distribution
endwalls removed from bottom, no bleed.

NB Note false origin

Bottom

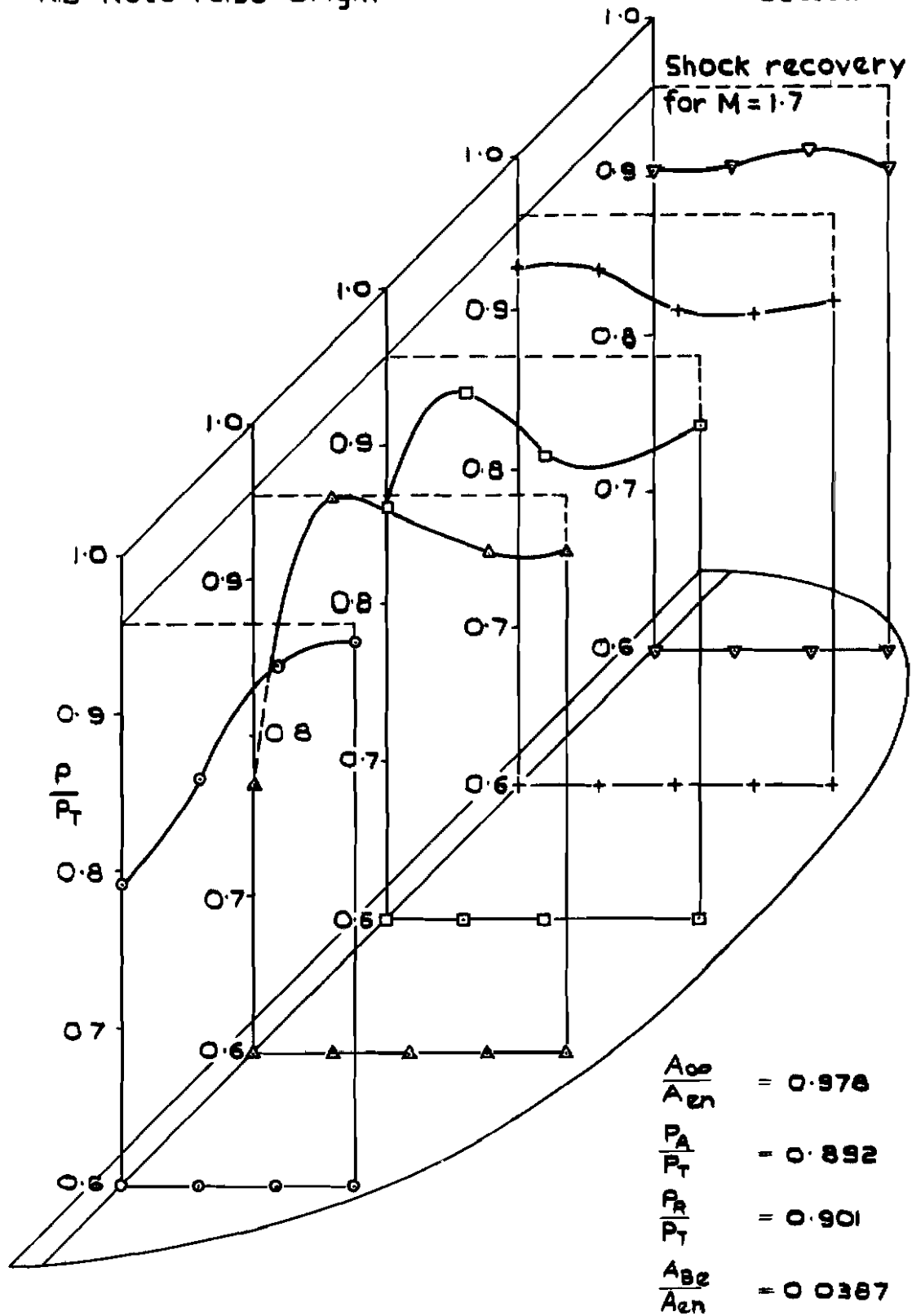


Fig.14 Duct pressure distribution.
endwalls removed from bottom, with bleed.

NB Note false origin

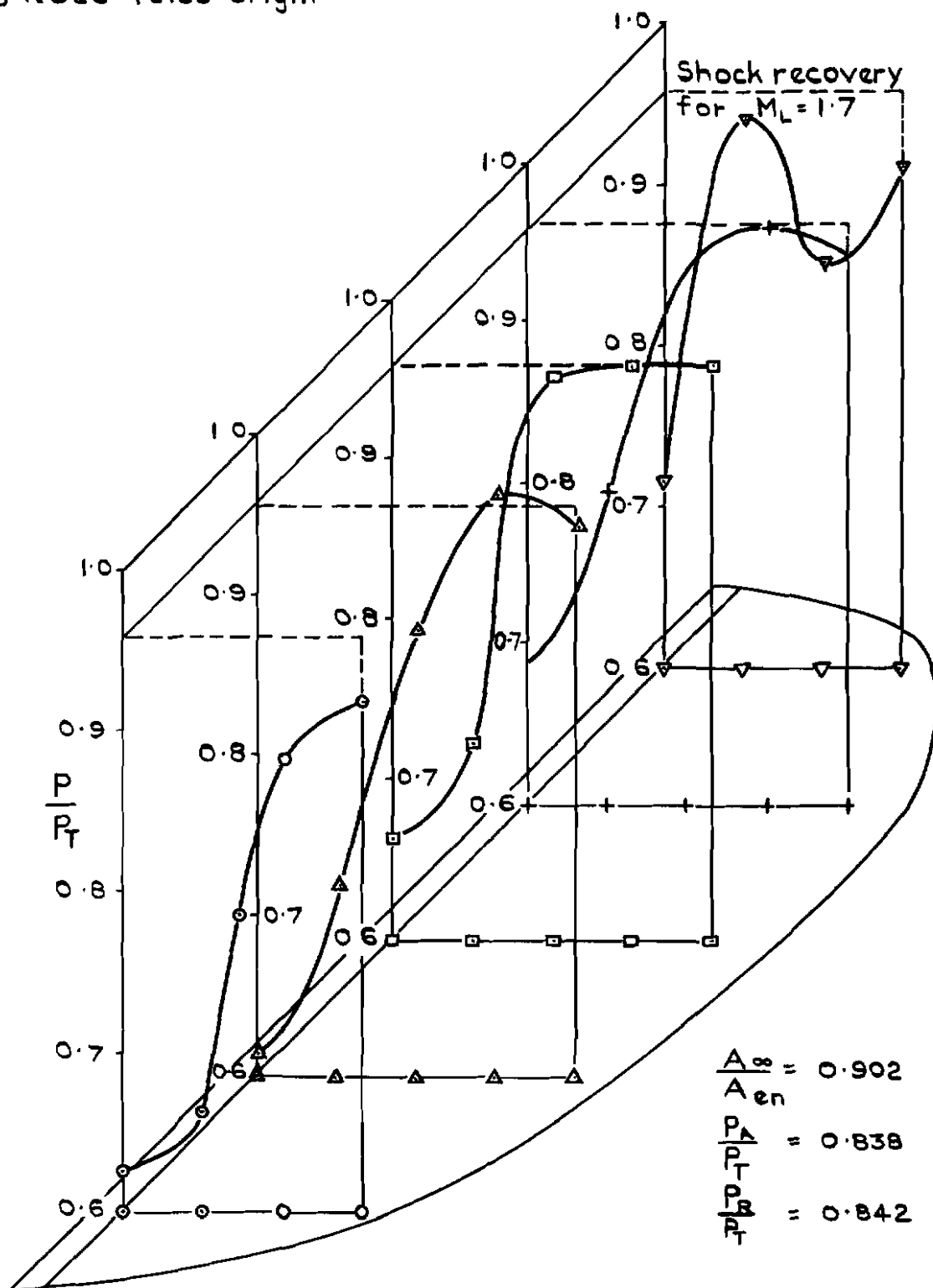


Fig.15 Duct pressure distribution no endwalls, no bleed.

NB Note false origin

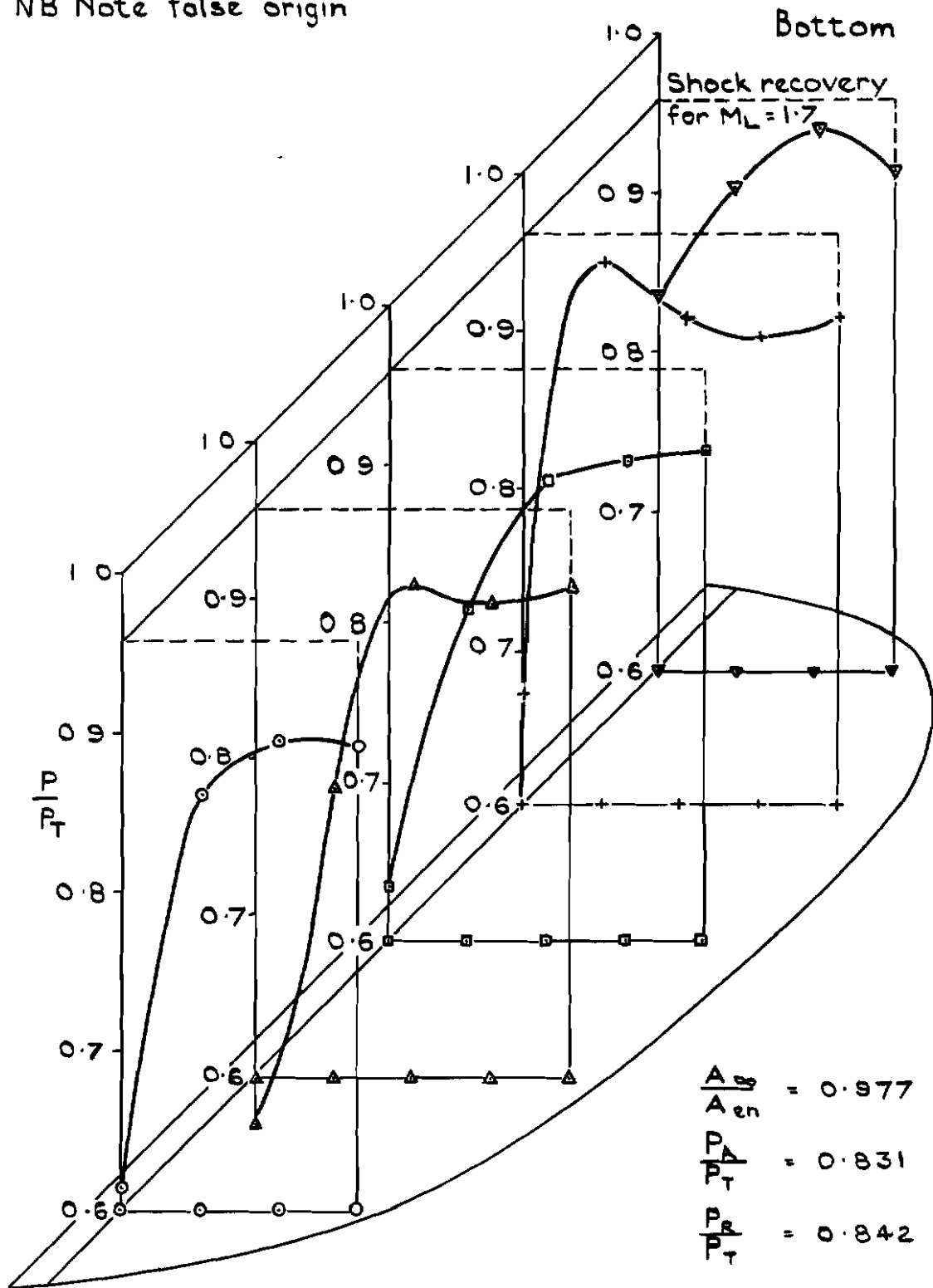
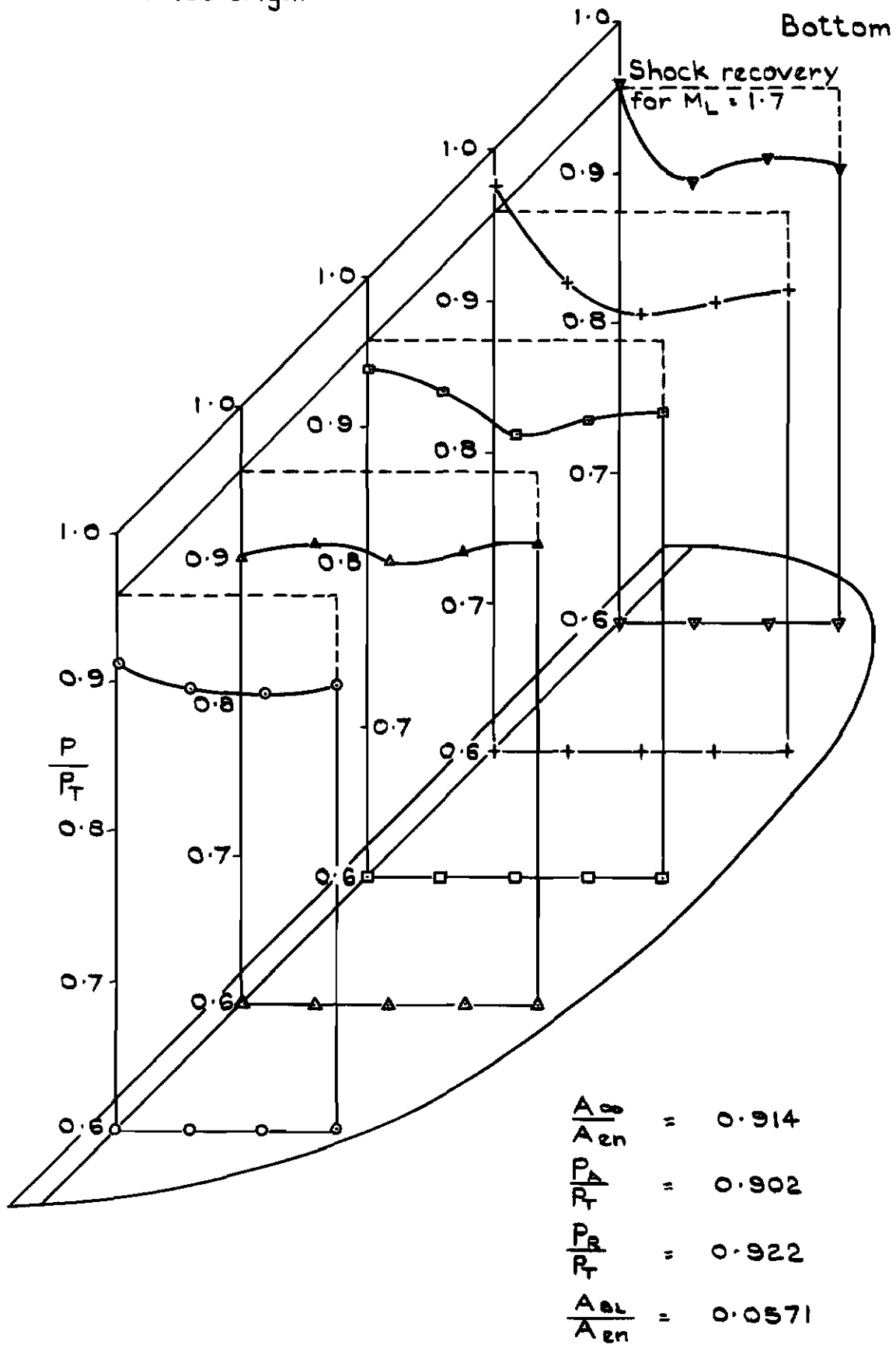


Fig 16 Duct pressure distribution no endwalls, no bleed

NB Note false origin



$$\frac{A_{\infty}}{A_{en}} = 0.914$$

$$\frac{P_A}{P_T} = 0.902$$

$$\frac{P_B}{P_T} = 0.922$$

$$\frac{A_{eL}}{A_{en}} = 0.0571$$

Fig.17 Duct pressure distribution no endwalls, with bleed

NB Note false origin

Bottom

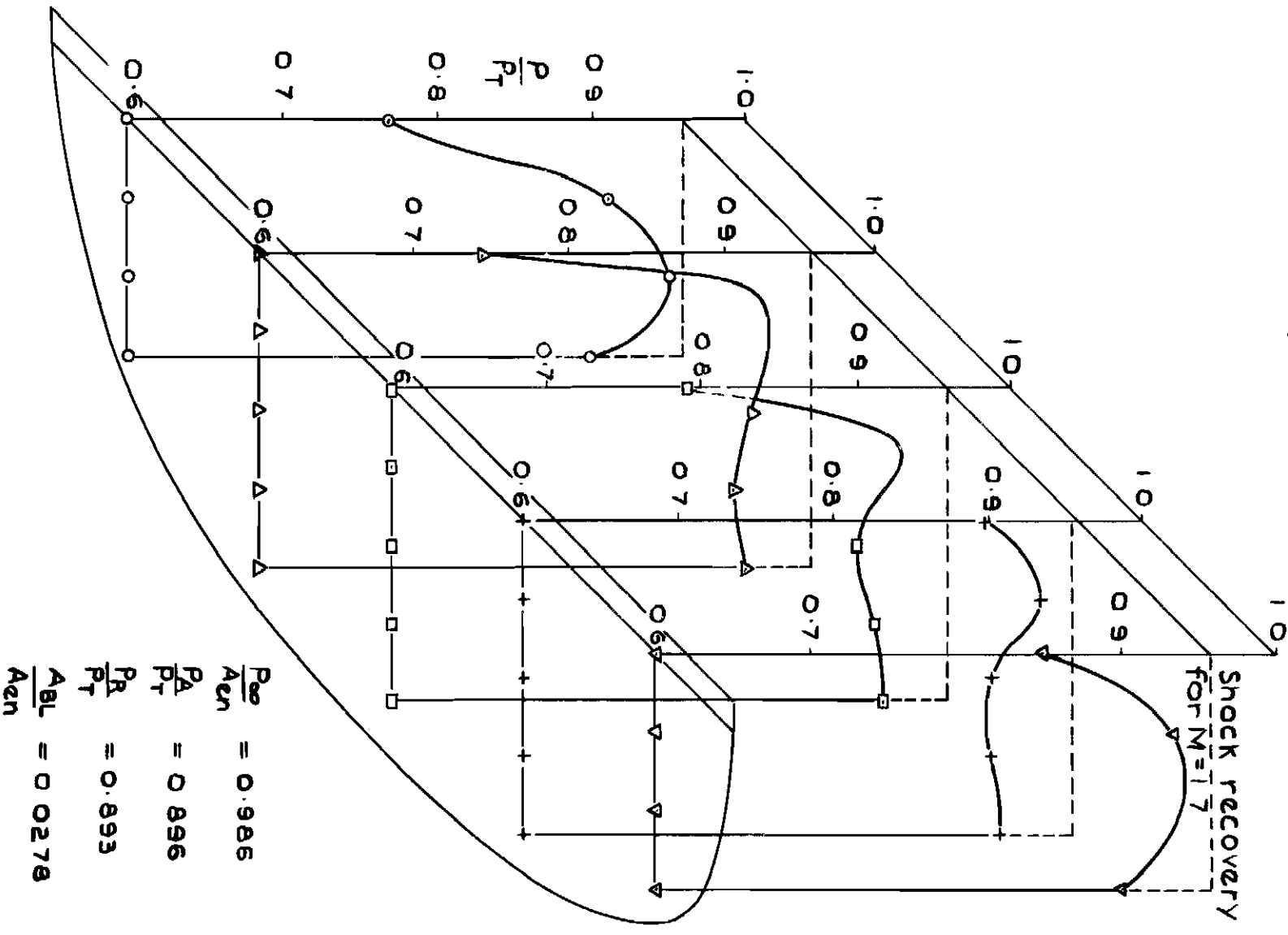


Fig 18 Duct pressure distribution no endwalls, with bleed.

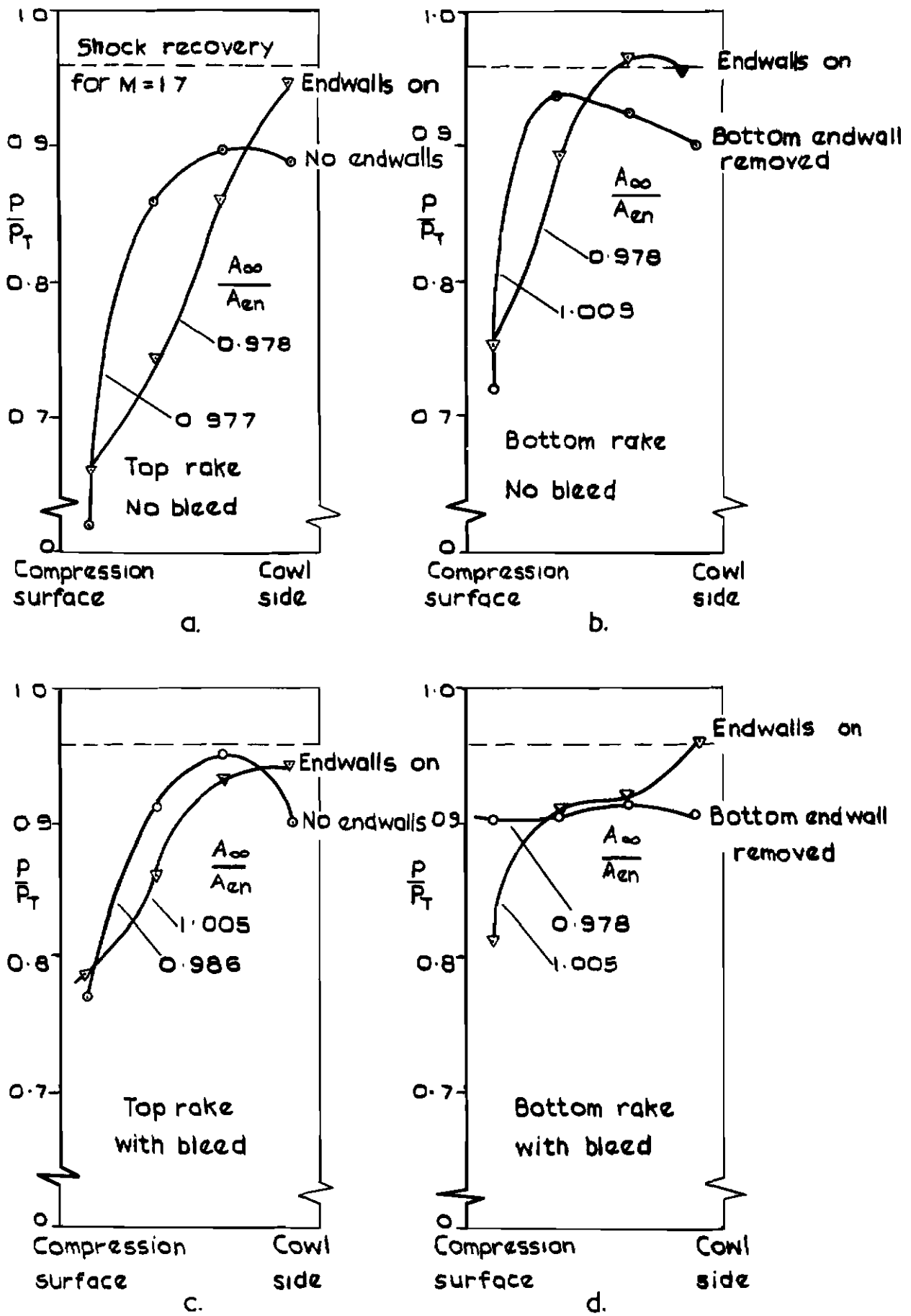


Fig. 19 Pressure distributions with and without endwalls

A.R.C. C.P.1026

March 1968

Shaw, M. M.

THE EFFECT AT $M = 1.7$ OF REMOVING SWEEPED ENDWALLS FROM
A WEDGE COMPRESSION INTAKE

Mean pressure recovery, distortion and the extent of stable subcritical flow have been measured at zero incidence on a fuselage side intake having a wedge compression surface. The intake was separated from the fuselage by a boundary layer diverter, and had a bleed on the compression surface just inside the entry plane. It was tested with and without bleed having top and bottom swept endwalls on, top endwalls on, and both endwalls off.

Detailed measurements of duct total pressure were made at 1.8 times the capture height downstream of the inlet plane for all configurations.

Removal of the endwalls leads to an increase in the uniformity of pressure distribution and to an increase in the range of stable subcritical flow.

533.697.2 :
533.694.73 :
533.6.011.5

A.R.C. C.P.1026

March 1968

Shaw, M. M.

THE EFFECT AT $M = 1.7$ OF REMOVING SWEEPED ENDWALLS FROM
A WEDGE COMPRESSION INTAKE

Mean pressure recovery, distortion and the extent of stable subcritical flow have been measured at zero incidence on a fuselage side intake having a wedge compression surface. The intake was separated from the fuselage by a boundary layer diverter, and had a bleed on the compression surface just inside the entry plane. It was tested with and without bleed having top and bottom swept endwalls on, top endwalls on, and both endwalls off.

Detailed measurements of duct total pressure were made at 1.8 times the capture height downstream of the inlet plane for all configurations.

Removal of the endwalls leads to an increase in the uniformity of pressure distribution and to an increase in the range of stable subcritical flow.

533.697.2 :
533.694.73 :
533.6.011.5

A.R.C. C.P.1026

March 1968

Shaw, M. M.

THE EFFECT AT $M = 1.7$ OF REMOVING SWEEPED ENDWALLS FROM
A WEDGE COMPRESSION INTAKE

Mean pressure recovery, distortion and the extent of stable subcritical flow have been measured at zero incidence on a fuselage side intake having a wedge compression surface. The intake was separated from the fuselage by a boundary layer diverter, and had a bleed on the compression surface just inside the entry plane. It was tested with and without bleed having top and bottom swept endwalls on, top endwalls on, and both endwalls off.

Detailed measurements of duct total pressure were made at 1.8 times the capture height downstream of the inlet plane for all configurations.

Removal of the endwalls leads to an increase in the uniformity of pressure distribution and to an increase in the range of stable subcritical flow.

533.697.2 :
533.694.73 :
533.6.011.5 :

© *Crown Copyright* 1968

Published by

HER MAJESTY'S STATIONERY OFFICE

To be purchased from

49 High Holborn, London w c 1

13A Castle Street, Edinburgh 2

109 St. Mary Street, Cardiff cf1 1JW

Brazennose Street, Manchester 2

50 Fairfax Street Bristol BS1 3DE

258 Broad Street, Birmingham 1

7 Linenhall Street, Belfast BT2 8AY

or through any bookseller